Environ Geochem Health (2020) 42:1569–1578
https://doi.org/10.1007/s10653-019-00458-5

ORIGINAL PAPER

Low-cost field production of biochars and their properties

Liang Xiao · Lirong Feng · Guodong Yuan · Jing Wei

Received: 14 February 2019 / Accepted: 29 October 2019 / Published online: 7 November 2019

Abstract Biochar has been intensively investigated for carbon sequestration, soil fertility enhancement, and immobilization of heavy metals and organic pollutants. Large-scale use of biochar in agricultural production and environmental remediation, however, has been constrained by its high cost. Here, we demonstrated the production of low-cost biochar ($20/ton) in the field from *Robinia pseudoacacia* biowaste via a combined aerobic and oxygen-limited carbonization process and a fire-water-coupled method. It involved aerobic combustion at the outer side of biomass, oxygen-limited pyrolysis in the inner core of biomass, and the termination of the carbonization by water spray. The properties of biochar thus produced were greatly affected by exposure time (the gap between a burning char fell to the ground and being extinguished by water spray). Biochar formed by zero exposure time showed a larger specific surface area (155.77 m^2/g), a higher carbon content (67.45%), a lower ash content (15.38%), and a higher content of carboxyl and phenolic-hydroxyl groups (1.74 and 0.86 mol/kg, respectively) than biochars formed with longer exposure times (5–30 min). Fourier-transform infrared spectroscopic (FTIR) spectra indicated that oxygen-containing functional groups of biochar played a role in Cd and oxytetracycline sorption though a quantitative relationship could not be established as the relative contribution of carbon and ash moieties of biochar to the sorption was unknown. Outcomes from this research provide an option for inexpensive production of biochar to support its use as a soil amendment in developing countries.

Keywords Biowaste · Exposure times · Functional groups · Cadmium · Oxytetracycline

L. Xiao · L. Feng · J. Wei
CAS Key Laboratory of Coastal Environmental Processes and Ecological Remediation, Yantai Institute of Coastal Zone Research, Chinese Academy of Sciences (CAS), Yantai, Shandong 264003, China

L. Xiao · L. Feng
University of Chinese Academy of Sciences, Beijing 100049, China

G. Yuan (✉)
School of Environmental and Chemical Engineering, Zhaoqing University, Zhaoqing, Guangdong 526061, China
e-mail: yuanguodong@zqu.edu.cn

Introduction

Terra preta, deep carbon-rich soil in the Amazon basin with a higher fertility and crop yield than surrounding soils, has stimulated investigations into its mysterious past (Marris 2006). The burning of plant residues by ancient Amazonian natives was believed the cause of the higher fertility and carbon content, and the latter considered to have the potential for carbon

sequestration (Harder 2006), which, in turn, has made biochar research a hotspot in environmental studies.

Biochar is a porous, carbon-rich material with a high specific surface area, abundant functional groups, and rich nutrients (Chagger et al. 1998; Antal and Gronli 2003; Lehmann 2007; Wang et al. 2013; Ahmad et al. 2014; Xiao et al. 2014). It is typically produced by pyrolysis of biowaste under limited oxygen conditions (Glaser et al. 2002; Kookana et al. 2011), and its properties are influenced by feedstock types, pyrolysis temperature, heating rate and residence time (Al-Wabel et al. 2018; Weber and Quicker 2018). In spite of policy promotion and intensive research in recent years on the beneficial use of biochar in agriculture and environmental remediation (Marris 2006; Houben et al. 2013; Zhang et al. 2013; Dai et al. 2017; Yang et al. 2018; Al-Wabel et al. 2019), biochar applications on large scale are rare (Zhou et al. 2018; Saifullah et al. 2018). The cost in association with the transportation of biowaste and biochar, equipment purchase, pyrolysis process, and high-use dosage often makes agricultural and environmental use of biochar infeasible (Blackwell et al. 2009; Marouš̆ek et al. 2017). In general, biochar may cost between $222 and $584/ton to produce, deliver, and spread on fields (Shackley et al. 2011; Huang et al. 2014; Shabangu et al. 2014; Ahmed et al. 2015), which is more than the profit improvement of $96.13/ton from biochar being used as soil amendment (Galinato et al. 2011; Campbell et al. 2018). Biochar as a commodity for agricultural use has been challengeable (Vochozka et al. 2016), prompting the development of methods for inexpensive biochar production (Saifullah et al. 2018).

If biochar could be produced in the field from local biowaste for local use, its transportation cost would be eliminated, and overall cost would be greatly reduced, thus making biochar use as a soil amendment more feasible. Filed production of biochar can be achieved via a couple of methods. The first method involved coupled oxygen-limiting and mist-spraying techniques, as reported by Xiao et al. (2019a), though its production efficiency is not very high. The second method is a result of a reconsideration of the preconceived notions of biochar production via pyrolysis of biowaste in the absence of oxygen. Inspired by charcoal production in nature, where wood and humus have been converted into charcoal by forest fire since time immemorial (Wardle et al. 2008), we hypothesized that biochar could be produced in the field by manipulating the pyrolysis of biowaste with fire and water. This hypothesis has been proven feasible via a combination of aerobic combustion on the exterior surface of biomass and oxygen-limited pyrolysis inside of the biomass in a brick-constructed trough and by using a fire-water-coupled method. Biochar was produced in the field at an estimated cost of $24/ton (Xiao et al. 2019b). Moving the brick-constructed trough to another area, however, is inconvenient. Thus, a simplified version is proposed here to produce biochar from biowaste by coordinating the use of fire and water. It involved three subprocesses: (1) open burning of a biomass stack to instantly reach a high temperature to mimic a high carbonization temperature and a fast heating rate in conventional pyrolysis where biomass is heated (Crombie et al. 2013); (2) oxygen-limiting pyrolysis in the inner core of biomass to form dark red char that subsequently fell to the ground; and (3) termination of pyrolysis in the fallen dark red char at a controlled time by water spray (Xiao et al. 2019b) to mimic the residence time in conventional pyrolysis. Thus, three parameters (heating rate, carbonization temperature, and residence time) that control the properties of biochar in conventional pyrolysis (Al-Wabel et al. 2018) have been simplified to a single operating parameter: exposure time, with a hypothesis that this single operating parameter can control biochar properties. Exposure time is the duration between a burning char fell to the ground and water spray was applied to terminate the pyrolysis.

In this study, *Robinia pseudoacacia* branch was used as a feedstock to produce biochar in the field via a combination of aerobic and oxygen-limited carbonization with a fire-water-coupled method. The purpose of this study was threefold: (1) to report a method for low-cost production of biochar in field; (2) to ascertain the influence of exposure time on biochar properties; and (3) to estimate the potential of the biochar to adsorb two common contaminants, cadmium (Cd) and oxytetracycline (OTC).

Materials and methods

Biochar production in the field

Biowaste pruned from *Robinia pseudoacacia* in Pucheng County, Shaanxi Province, was used as

feedstock for biochar production. The air-dried branches were 0.2–0.6 m long, with a diameter of 0.8–4.5 cm, and water content of 11.38 ± 0.15%.

The feedstock was converted to biochar via a combination of aerobic and oxygen-limited carbonization processes. Briefly, *Robinia pseudoacacia* branches were randomly piled into stacks of 1.5 m long and 0.6 m high, with a trapezoidal cross section. Two groups, each with five random stacks, were used as duplicated treatments. The stacks were first ignited from four sides to start an aerobic burning process to reach a high temperature instantly. Occurring inside the branches was oxygen-limited pyrolysis that turned the feedstock to dark red char. It was named oxygen-limited for two reasons: oxygen of the feedstock (e.g., in carbohydrate) could still be consumed in the pyrolysis and oxygen diffusion from outside to the core of feedstock could not be excluded. The dark red char was knocked down to the ground, collected by using a fork and shovel, and water-mist sprayed to extinguish either immediately (i.e., exposure time = 0) or after 5, 10, 15 and 30 min of exposure to the air (exposure time = 5, 10, 15 and 30 min). The formed biochars were labeled as I, II, III, IV, and V, respectively (Fig. 1).

Pyrolysis termination temperature, defined as the temperature on the surface of the dark red char on the ground before water spray starts, was measured with a non-contact infrared thermometer (DT-8833, Beijing Huashengchang) with a range of − 50 to 800 °C and a resolution of 0.1 °C. The obtained biochar was oven-dried at 85 °C and then ground to pass through a 100-mesh sieve for laboratory analysis and sorption experiment.

The above combination of aerobic and oxygen-limited carbonization processes inevitably produced smoke, particularly at the initial stage. If required, this problem is solvable by a combination of physical filtering of large particles, high-voltage electric burning of small charcoal particles, and sorption of gases by a mud suspension to control the emissions of particulate matter (PM 2.5 and PM 10) and volatile organic matter to meet environmental standard (Xiao et al. 2019b).

Cadmium sorption experiment

Cadmium solutions: 0.2747 g of cadmium nitrate ($Cd(NO_3)_2{\cdot}4H_2O$, analytical purity) was dissolved in deionized water to a volume of 100 mL to prepare a stock solution with a Cd(II) concentration of 1 g/L. It was used to make a working solution that contained 50 mg Cd/L and 1 mM $NaNO_3$ as a background electrolyte for use in Cd sorption experiment.

Sorption experiment was carried out in duplicate with blanks and controls. Briefly, 0.040 g of biochar with different exposure times were weighed into 50 mL centrifuge tubes that contained 40 mL solution of 50 mg Cd/L and 1 mM $NaNO_3$. The tubes were capped, shaken at 300 rpm in an oscillator at 25 °C for 24 h, and then centrifuged at 4000 rpm for 10 min. The supernatant was filtered through a 0.45 μm

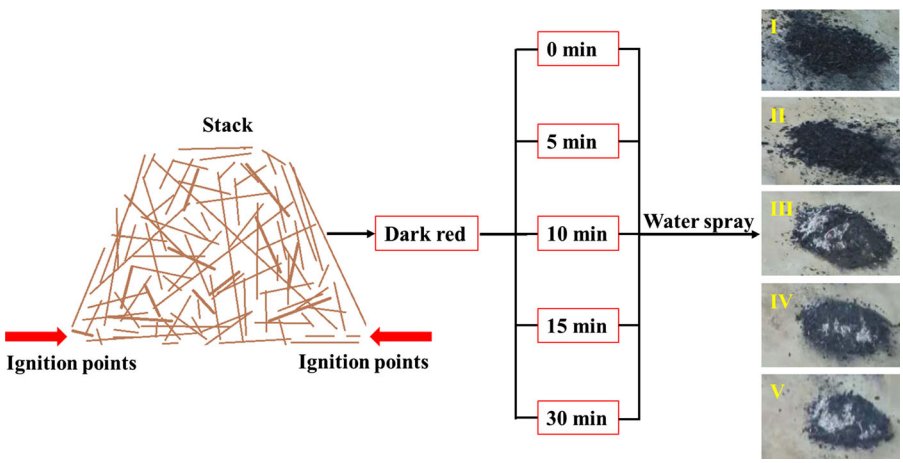

Fig. 1 Diagrams of low-cost biochar production in the field via a combination of aerobic and oxygen-limited carbonization with different exposure times

membrane for Cd concentration analysis by an atomic absorption spectrophotometer (Shimadzu, AA-7000). The residue in tubes was freeze-dried for Fourier-transform infrared spectroscopy (FTIR) analysis. The amount of sorbed Cd was calculated from the difference between the initial and equilibrium concentrations of Cd.

Oxytetracycline sorption experiment

Oxytetracycline solutions: 0.5000 g of OTC was dissolved in a methanol solution, diluted to 500 mL to obtain 1 g/L OTC stock solution, sealed, and stored in a refrigerator at 4 °C. 0.5850 g of NaCl and 0.1 g of NaN_3 (an inhibitor to avoid OTC biodegradation) were dissolved in Milli-Q water and diluted to 1 L to obtain 0.01 M NaCl background electrolyte solution.

Sorption experiment was carried out in duplicate with blanks and controls. Briefly, 0.040 g of biochar with different exposure times were weighted into 50 mL centrifuge tubes that contained 40 mL solution of 50 mg OTC/L and 0.01 M NaCl as background electrolyte. The capped tubes were shaken at 120 rpm at 25 °C for 24 h and then centrifuged at 4000 rpm for 10 min. The supernatant was filtered through a 0.45 μm membrane to determine OTC concentrations via a UV–Vis spectrophotometer (Thermo Genesys 10S) at a wavelength of 276 nm. The residue in tubes was freeze-dried for FTIR analysis. The amount of sorbed OTC was calculated from the difference between the initial and equilibrium concentrations of OTC.

Analytical methods

The ash content of biochar was determined by ignition in a muffle furnace at 800 °C for 4 h (Bao 2000). The pH of biochar was measured with deionized water at a ratio of 1:5 (w/v, shaking at 160 r/min for 24 h) using a pH meter (Five Easy Plus, METTLER TOLEDO). Elemental compositions of biochar were determined by an elemental analyzer (Vario Micro cube, Elementar). Functional groups of biochar were characterized by FTIR (Thermo Fisher Nicolet iS5) with a scan range of 500–4000 cm^{-1} and a resolution of 2.0 cm^{-1} (Wang 2013). Oxygen-containing functional groups were determined by the titration method of the International Humic Substances Society (http://humic-substances.org/) (International Humic Substances Society (IHSS) 2019). Specific surface area (SSA) was analyzed by the nitrogen sorption BET method on a fully automatic specific surface area and pore size distribution analyzer (Autosorb-iQ, Quantachrome).

Data processing

Excel 2010, SPSS 16.0, and Origin 8.0 were used for calculation, data analysis, and figure drawing. One-way ANOVA was performed for statistical significance analysis (Duncan's test) of the biochar properties.

Results and discussion

The combination of aerobic and oxygen-limited carbonization process

The burning process of *Robinia pseudoacacia* branches could be divided into three stages (Shafizadeh 1982; Hamelinck et al. 2005): (1) surface charred immediately but with an unburned core; (2) surface grayed out, the core was in a self-ignition state with high temperature and limited oxygen, and dark red char fell to the ground; and (3) the dark red char gradually burned out and became ash. Spraying water on the dark red char prevented the occurrence of the 3rd stage, thus favoring the formation of biochar instead of ash.

To help understand this effect, we can conceive a *Robinia pseudoacacia* branch as a miniature furnace: the outer part of the branch is similar to the furnace wall, whereas the inner core is equivalent to the biomass in the furnace. In other words, the carbonization process is a combination of surface combustion and oxygen-limited pyrolysis at the inner core.

The aerobic and oxygen-limited carbonization differs from the traditional pyrolysis in three aspects. First, the temperature is raised instantly in the former rather than slowly in the latter (Manyà 2012). Second, the residence time is much shorter in aerobic and oxygen-limited carbonization than in conventional pyrolysis (Crombie et al. 2013). A water spray immediately terminates the carbonization in aerobic and oxygen-limited method, whereas in conventional pyrolysis the carbonization lasts for hours. Third, a single operating parameter, exposure time, is used to

control the properties of the formed biochar in aerobic and oxygen-limited method, whereas in conventional pyrolysis three parameters (heating rate, temperature, and residence time) are combined to affect biochar properties.

The effect of exposure time on biochar properties

As shown in Fig. 2, all biochars produced with different exposure times were alkaline (pH from 9.42 to 9.49), with no significant difference. In contrast, as exposure time increased from 0 to 30 min pyrolysis termination temperature gradually decreased from 523.0, 493.4, 446.7, 402.4 to 238.3 °C, accompanied by an increase in ash content from 15.38, 23.40, 29.32, 36.64 to 48.45%. This negative effect of exposure time on biochar formation was further evidenced by a decrease in C, N, H, and S contents of biochar with the increasing exposure time

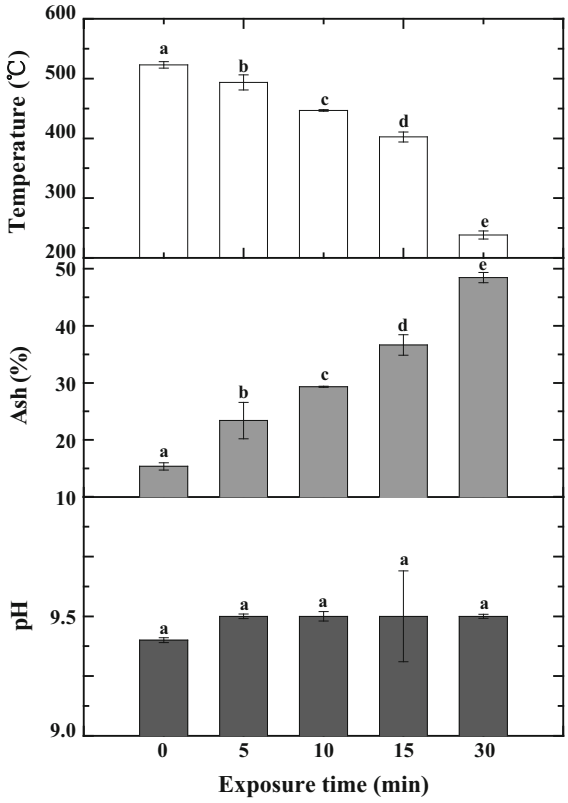

Fig. 2 Effect of exposure time on pyrolysis termination temperature and biochar properties. Different lower-case letters indicate significant differences between treatments ($p < 0.05$, Duncan's test)

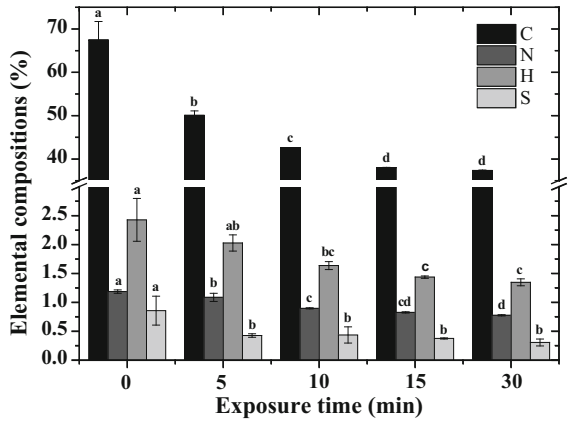

Fig. 3 The effect of exposure time on elemental compositions of biochars. Different lower-case letters indicate significant differences between treatments ($p < 0.05$, Duncan's test)

(Fig. 3). C, N, H, and S contents at 0 min of exposure time were the highest (67.45%, 1.19%, 2.43%, and 0.86%, respectively), and a significant difference was observed between 0 and 5 min. As exposure time increased, these elements converted to carbon, nitrogen, and sulfur oxide gases, resulting in biochars with a lighter color. As the C content of biochar formed at 0 min of exposure time was 67.45%, it could be classified as class 1 according to both European Biochar Certificate (EBC) Version 4.8 and International Biochar Initiative (IBI) Biochar Standards Version 2.0 (Campbell et al. 2018).

Figure 4 indicates that the SSA of biochars, an important indicator of their adsorptive capacity,

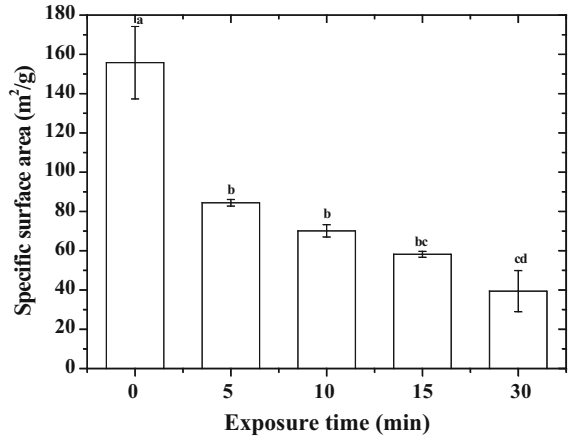

Fig. 4 Effect of exposure time on the specific surface area of biochars. Different lower-case letters indicate significant differences between treatments ($p < 0.05$, Duncan's test)

gradually decreased with exposure time. The decrease was most evident (41.7%) in the 0–5 min period. Generally speaking, a larger SSA indicated more pores and a better sorption performance (Joseph et al. 2009). The SSA of the biochar with 0 min exposure time was highest (155.77 m^2/g), suggesting its good adsorptive capacity than others (Genuino et al. 2018).

A higher pyrolysis temperature usually produces biochar with a larger SSA and pore volume (Keiluweit et al. 2010). Figure 2 shows that pyrolysis termination temperature at 0 min exposure time was the highest (523 °C), resulting in fluffy biochar with a porous structure (Fig. 5), lightweight, and a large SSA (155.77 m^2/g). With a rise in exposure time, aerobic combustion lasted longer, causing the collapse of the carbon skeleton, the filling of pores by ash, and a decrease in SSA. It is conceivable that if exposure time further increased, the end product would be ash. At 70 min of exposure time, the ask-like product had a SSA of 10.23 m^2/g, much lower than those of biochars formed at 0 to 30 min of exposure times. After comparing 93 biochar samples, Yuan et al. (2016) found that the SSA of most wood biochar was below 100 m^2/g. According to EBC Version 4.8 and IBI Biochar Standards Version 2.0 (Campbell et al. 2018), biochar formed at 0 min of exposure time was preferable.

Figure 6 shows that phenolic-hydroxyl and carboxyl groups of biochar significantly decreased with exposure time from 0 to 10 min. Their contents were highest at 0 min, being 0.86 mol/kg for phenolic-OH and 1.74 mol/kg for –COOH groups. Due to their roles in ion exchange, sorption, and the complexation of metal and organic pollutants, oxygen-containing functional groups of biochar indicate its sorption ability (Chen et al. 2008). Phenolic-hydroxyl and carboxyl groups, formed during the oxygen-limiting thermal cracking process of *Robinia pseudoacacia* branches, were consumed as exposure time increased.

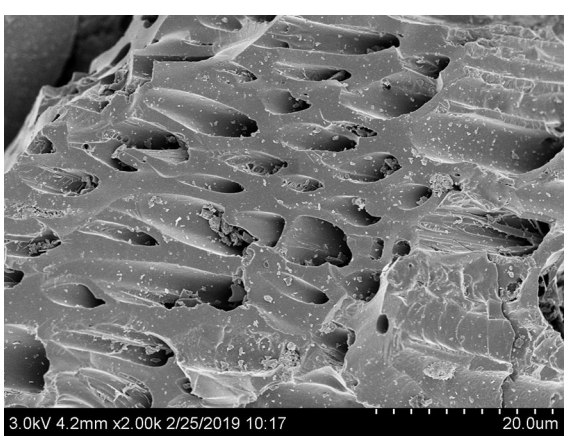

Fig. 5 SEM image of biochar produced in 0 min of exposure time

Effect of exposure time on biochar to sorb Cd and OTC

Cd sorption on biochar first decreased and then increased with exposure time (Fig. 7), and the sorption capacities were higher at 0 and 30 min than between. The sorption capacity of this research was similar to those of wood biochars (0.3–5.5 mg/g), as Inyang et al. (2016) summarized. Cautions, however, should be exercised in comparing sorption capacities as they depend on experimental conditions (e.g., pH, co-existing ions). Estimating sorption capacity from a single concentration sorption experiment provides a convenient way for fast screening of adsorbents, as routinely done in soil testing of phosphorus sorption potential.

As Oliveira et al. (2017) and Wu et al. (2019) summarized, metal ion immobilization by biochar involves mechanisms of (i) electrostatic attraction between cationic heavy metals and negatively charged minerals on biochars; (ii) cation exchange between metal ions and mineral ions on biochars; (iii) complexation of metals with surface functional groups of biochars; and (iv) precipitation of heavy metals with biochar minerals (e.g., SiO_3^{2-}, PO_4^{3-}, OH^-, CO_3^{2-}). At 0 and 5 min of exposure times the ash content of biochar (15.38%, 23.40%) was low, so was its contribution to Cd sorption. The high oxygen-containing functional groups of biochar at 0 min would favor Cd sorption through complexation or ion exchange. At exposure times of 10, 15, and 30 min, the sum of –COOH and phenolic-OH groups, being 1.94, 1.92, and 1.94 mol/kg, respectively, was about the same, but the corresponding ash content increased to 29.32, 36.64 and 48.45%. The high ash content promoted Cd sorption onto biochar, as Inyang et al. (2016) and Hass and Lima (2018) reported. Further, the high pH (9.42–9.49) would favor Cd precipitation. Similarly, Wei et al. (2019b) reported that high ash content and pH contributed to Cu sorption by halophyte biochar via precipitation and formation of

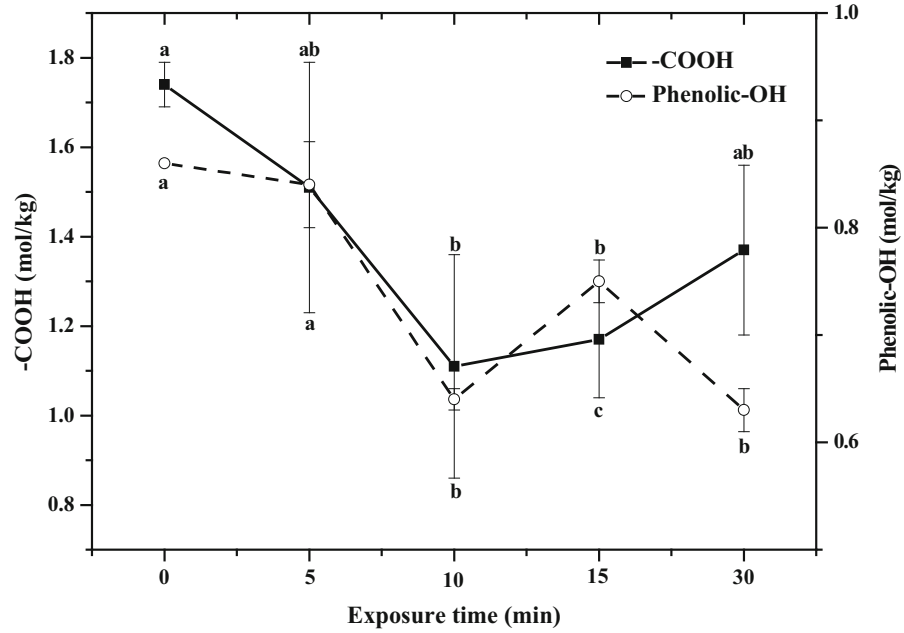

Fig. 6 Effect of exposure time on –COOH and phenolic-OH contents of biochars. Different lower-case letters indicate significant differences between treatments ($p < 0.05$, Duncan's test)

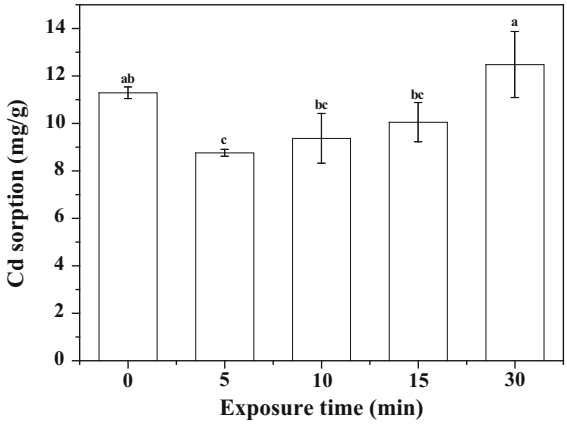

Fig. 7 Effect of exposure time on Cd sorption by biochars. Different lower-case letters indicate significant differences between treatments ($p < 0.05$, Duncan's test)

mineral langite. Overall, functional groups and ash content of biochar jointly affect Cd sorption (Singh and Prasad 2015).

The FTIR spectra of biochar before and after Cd sorption are shown in Fig. 9. The assignment of the peaks was based on the work of Singh and Prasad (2015) and Wei et al. (2019a, c). After Cd sorption the peak of phenolic-OH functional group at 3740 cm^{-1} disappeared, and the peaks of –COOH functional group at 1700 cm^{-1} and the C=O/C=C functional group at 1570 cm^{-1} moved toward low wavenumbers (i.e., red shift occurred), which indicates that oxygen-containing functional groups play an important role in Cd sorption by biochar.

OTC sorption on biochar was highest at 0 min exposure time, and it decreased with rising exposure time (Fig. 8). The sorption capacities were similar to those of other wood biochars (Zhang and Wang 2018; Dai et al. 2019). Again, caution is required in the direct comparison of sorption capacities from different experimental conditions. The sorption trend agreed

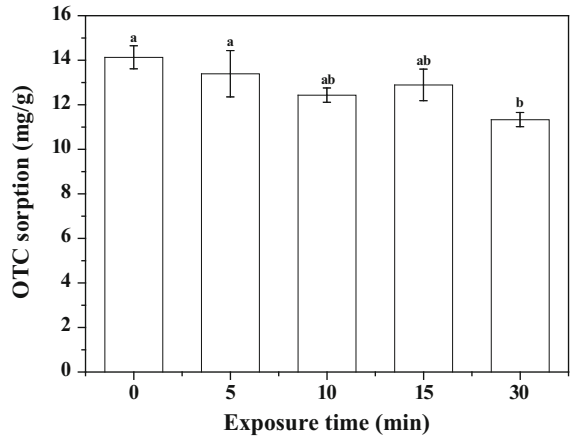

Fig. 8 Effect of exposure time on OTC sorption by biochars. Different lower-case letters indicate significant differences between treatments ($p < 0.05$, Duncan's test)

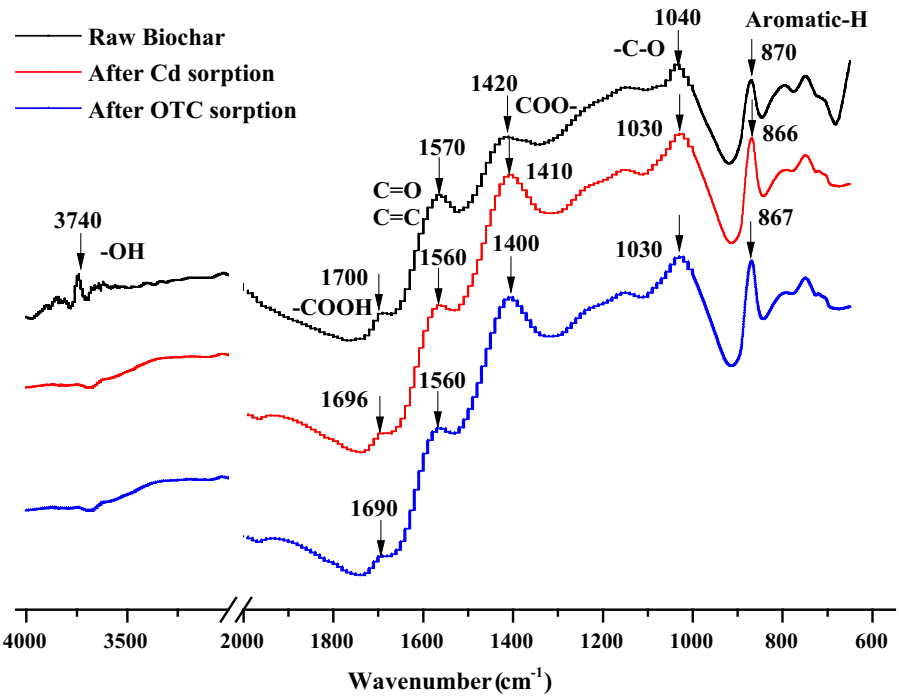

Fig. 9 FTIR spectra of biochar from 0 min exposure time before and after Cd or OTC sorption

with the SSA of biochars (Fig. 4) and the contents of –COOH and phenolic-OH groups (Fig. 6). As OTC is a bulky molecule its sorption on biochar is enhanced by a large SSA for pore filling, and H-bonding is the dominant mechanism for the sorption (Fu et al. 2016).

The FTIR spectra (Fig. 9) show that after OTC sorption the absorption peaks of structural groups of biochar at 0 min exposure time either disappeared (phenolic-OH functional group) or moved to lower wavenumbers (–COOH and C=O/C=C functional groups). These changes indicate the formation of hydrogen bonds and the existence of π-π electron donor-acceptor interactions (Ji et al. 2011; Fu et al. 2016), and are consistent with the reports of Ahmed et al. (2016, 2017).

Conclusions and prospects

Inspired by the charcoal formation in nature, we have proved that low-cost biochar can be produced in field by the combination of aerobic and oxygen-limited carbonization of *Robinia pseudoacacia* branches, involving combustion at the outer side of biomass, oxygen-limited pyrolysis in the inner core of biomass, and the termination of the pyrolysis by water spray. The properties of obtained biochars could be adjusted by a single factor—exposure time, the duration between burning char fell to the ground and water was sprayed to extinguish. In other words, water spray inhibits further carbonization of dark red char and forms biochar. Biochar formed by a fast termination (0 min exposure time) showed a larger specific surface area (155.77 m^2/g), higher contents of carbon content (67.45%), carboxyl (1.74 mol/kg), and phenolic-hydroxyl groups (0.86 mol/kg), and a lower ash content (15.38%) than biochars formed from a slow termination (5–30 min of exposure time). As this aerobic and oxygen-limited carbonization method eliminated transportation and equipment costs, biochars could be produced in a village of northwestern China at $20/ton. This research may help accelerate a paradigm shift in biochar production from a sophisticated stationary facility to a simple method for practical use in the field. Low-cost is a great advantage that would help agricultural and environmental applications of biochar.

Acknowledgements This work was supported by grants from the Chinese National Key Research and Development Program (2016YFD0200303), Key Research and Development Program

of Shandong Province (2016CYJS05A01), and the National Natural Science Foundation of China (41501522). Mr. Guanhua Shen of Zhaoqing University is appreciated for analyzing the specific surface area of biochar. We are grateful to Anne Austin, Manaaki Whenua—Landcare Research, New Zealand, for editing the original manuscript, and to three anonymous reviewers for their constructive comments and suggestions.

References

Ahmad, M., Rajapaksha, A. U., Lim, J. E., Zhang, M., Bolan, N., Mohan, D., et al. (2014). Biochar as a sorbent for contaminant management in soil and water: A review. *Chemosphere, 99*(3), 19–33.

Ahmed, M. B., Zhou, J. L., Ngo, H. H., & Guo, W. S. (2015). Adsorptive removal of antibiotics from water and wastewater: progress and challenges. *Science of the Total Environment, 532,* 112–126.

Ahmed, M. B., Zhou, J. L., Ngo, H. H., Guo, W. S., & Chen, M. F. (2016). Progress in the preparation and application of modified biochar for improved contaminant removal from water and wastewater. *Bioresource Technology, 214,* 836–851.

Ahmed, M. B., Zhou, J. L., Ngo, H. H., Guo, W. S., Johir, M. A. H., & Sornalingam, K. (2017). Single and competitive sorption properties and mechanism of functionalized biochar for removing sulfonamide antibiotics from water. *Chemical Engineering Journal, 311*(1), 348–358.

Al-Wabel, M. I., Hussain, Q., Usman, A. R. A., Ahmad, M., Abduljabbar, A., Sallam, A. S., et al. (2018). Impact of biochar properties on soil conditions and agricultural sustainability: a review. *Land Degradation & Development*, *29*(7), 2124–2161.

Al-Wabel, M. I., Usman, A. R., Al-Farraj, A. S., Ok, Y. S., Abduljabbar, A., Al-Faraj, A. I., et al. (2019). Date palm waste biochars alter a soil respiration, microbial biomass carbon, and heavy metal mobility in contaminated mined soil. *Environmental Geochemistry and Health*, *41*(4), 1705–1722.

Antal, M. J., & Gronli, M. (2003). The art, science, and technology of charcoal production. *Industrial and Engineering Chemistry Research, 42*(8), 1619–1640.

Bao, S. D. (2000). *Soil agrochemical analysis* (pp. 258–260). Beijing: China Agriculture Press.

Blackwell, P., Reithmuller, G., & Collins, M. (2009). Biochar application to soil. In J. Lehmann & S. Joseph (Eds.), *Biochar for environmental management: Science and technology* (pp. 207–226). London: Earthscan.

Campbell, R. M., Anderson, N. M., Daugaard, D. E., & Naughton, H. T. (2018). Financial viability of biofuel and biochar production from forest biomass in the face of market price volatility and uncertainty. *Applied Energy, 230,* 330–343.

Chagger, H. K., Kendall, A., McDonald, A., Pourkashanian, M., & Williams, A. (1998). Formation of dioxins and other semi-volatile organic compounds in biomass combustion. *Applied Energy, 60*(2), 101–114.

Chen, B. L., Zhou, D. D., & Zhu, L. Z. (2008). Transitional adsorption and partition of nonpolar and polar aromatic contaminants by biochar of pine needles with different pyrolytic temperatures. *Environmental Science and Technology, 42*(14), 5137–5143.

Crombie, K., Mašek, O., Sohi, S. P., Brownsort, P., & Cross, A. (2013). The effect of pyrolysis conditions on biochar stability as determined by three methods. *Global Change Biology Bioenergy, 5*(2), 122–131.

Dai, Z. M., Zhang, X., Tang, C., Muhammad, N., Wu, J. J., Brookes, P. C., et al. (2017). Potential role of biochar in decreasing soil acidification A critical review. *Science of the Total Environment, 581–582,* 601–611.

Dai, Y. J., Zhang, N. X., Xing, C. M., Cui, Q. X., & Sun, Q. Y. (2019). The adsorption, regeneration and engineering applications of biochar for removal organic pollutants: A review. *Chemosphere, 223,* 12–27.

Fu, B. M., Ge, C. J., Yue, L., Luo, J. W., Feng, D., Deng, H., et al. (2016). Characterization of biochar derived from pineapple peel waste and its application for adsorption of oxytetracycline from aqueous solution. *BioResources, 11*(4), 9017–9035.

Galinato, S., Yoder, J., & Granatstein, D. (2011). The economic value of biochar in crop production and carbon sequestration. *Energy Policy, 39,* 6344–6350.

Genuino, D. A., De Luna, M. D., & Capareda, S. C. (2018). Improving the surface properties of municipal solid waste-derived pyrolysis biochar by chemical and thermal activation: optimization of process parameters and environmental application. *Waste Management, 72,* 255–264.

Glaser, B., Lehmann, J., & Zech, W. (2002). Ameliorating physical and chemical properties of highly weathered soils in the tropics with charcoal-a review. *Biology and Fertility of Soils, 35*(4), 219–230.

Hamelinck, C. N., Hooijdonk, G. V., & Faaij, A. P. C. (2005). Ethanol from lignocellulosic biomass: techno-economic performance in short-, middle- and long-term. *Biomass and Bioenergy, 28*(4), 384–410.

Harder, B. (2006). Smoldered-earth policy: Created by ancient Amazonian natives, fertile, dark soils retain abundant carbon. *Science, 169*(9), 133.

Hass, A. & Lima, I. M. (2018). Effect of feed source and pyrolysis conditions on properties and metal sorption by sugarcane biochar. *Environmental Technology & Innovation*, *10*, 16–26.

Houben, D., Evrard, L., & Sonnet, P. (2013). Beneficial effects of biochar application to contaminated soils on the bioavailability of Cd, Pb and Zn and the biomass production of rapeseed (*Brassica napus* L.). *Biomass and Bioenergy, 57*(11), 196–204.

Huang, Y., Anderson, M., Lyons, G. A., McRoberts, W. C., Wang, Y. D., McIlveen-Wright, D. R., et al. (2014). Techno-economic analysis of biochar production and energy generation from poultry litter waste. *Energy Procedia, 61,* 714–717.

International Humic Substances Society (IHSS). https://www.humicsubstances.org/acidity.html. Accessed on 12 February 2019.

Inyang, M. I., Gao, B., Yao, Y., Xue, Y. W., Zimmerman, A., Mosa, A., et al. (2016). A review of biochar as a low-cost adsorbent for aqueous heavy metal removal. *Critical Reviews in Environmental Science and Technology, 46*(4), 406–433.

Ji, L. L., Wan, Y. Q., Zheng, S. R., & Zhu, D. Q. (2011). Adsorption of tetracycline and sulfamethoxazole on crop residue-derived ashes: Implication for the relative importance of black carbon to soil sorption. *Environmental Science and Technology, 45*(13), 5580–5586.

Joseph, S., Peacocke, C., Lehmann, J., & Munroe, P. (2009). Developing a biochar classification system and test methods. In J. Lehmann & S. Joseph (Eds.), *Biochar for environmental management* (pp. 107–126). London: Earthscan.

Keiluweit, M., Nico, P., Johnson, M. G., & Kleber, M. (2010). Dynamic molecular structure of plant biomass-derived black carbon (Biochar). *Environmental Science and Technology, 44*(4), 1247–1253.

Kookana, R. S., Sarmah, A. K., Zwieten, L. V., Krull, E., & Singh, B. (2011). Biochar application to soil: agronomic and environmental benefits and unintended consequences. *Advances in Agronomy, 112,* 103–143.

Lehmann, J. (2007). A handful of carbon. *Nature, 447*(7141), 143–144.

Manyà, J. J. (2012). Pyrolysis for biochar purposes: A review to establish current knowledge gaps and research needs. *Environmental Science and Technology, 46,* 7939–7954.

Marousěk, J., Vochozka, M., Plachý, J., & Žák, J. (2017). Glory and misery of biochar. *Clean Technologies and Environmental Policy, 19,* 311–317.

Marris, E. (2006). Putting the carbon back: Black is the new green. *Nature, 442*(7103), 624–626.

Oliveira, F. R., Patel, A. K., Jaisi, D. P., Adhikari, S., Lu, H., & Khanal, S. K. (2017). Environmental application of biochar: Current status and perspectives. *Bioresource Technology, 246,* 110–122.

Saifullah, Dahlawi, S., Naeem, A., Rengel, Z., & Naidu, R. (2018). Biochar application for the remediation of salt-affected soils: Challenges and opportunities. *Science of the Total Environment*, *625*, 320–335.

Shabangu, S., Woolf, D., Fisher, E. M., Angenent, L. T., & Lehmann, J. (2014). Techno-economic assessment of biomass slow pyrolysis into different biochar and methanol concepts. *Fuel, 117,* 742–748.

Shackley, S., Hammond, J., Gaunt, J., & Ibarrola, R. (2011). The feasibility and costs of biochar deployment in the UK. *Carbon Management, 2*(3), 335–356.

Shafizadeh, F. (1982). Introduction to pyrolysis of biomass. *Journal of Analytical and Applied Pyrolysis, 3,* 283–305.

Singh, A., & Prasad, S. M. (2015). Remediation of heavy metal contaminated ecosystem: An overview on technology advancement. *International Journal of Environmental Science and Technology, 12,* 353–366.

Vochozka, M., Marouskova, A., Vachal, J., & Strakova, J. (2016). Biochar pricing hampers biochar farming. *Clean Technologies and Environmental Policy, 18*(4), 1225–1231.

Wang, Q. (2013). *Influence of biomass feedstocks and production temperatures on the structure-activities of biochar*. Shanghai: Shanghai Jiao Tong University, PhD. Thesis, pp 12–13.

Wang, C., Lu, H. H., Dong, D., Deng, H., Strong, P. J., Wang, H. L., et al. (2013). Insight into the effects of biochar on manure composting: Evidence supporting the relationship between N_2O emission and denitrifying community. *Environmental Science and Technology, 47*(13), 7341–7349.

Wardle, D. A., Nilsson, M. C., & Zackrisson, O. (2008). Fire-derived charcoal causes loss of forest humus. *Science, 320,* 2.

Weber, K., & Quicker, P. (2018). Properties of biochar. *Fuel, 217,* 240–261.

Wei, J., Tu, C., Yuan, G. D., Bi, D. X., Wang, H. L., Zhang, L. J., et al. (2019a). Pyrolysis temperature-dependent changes in the characteristics of biochar-borne dissolved organic matter and its copper binding properties. *Bulletin of Environmental Contamination and Toxicology, 103,* 169–174.

Wei, J., Tu, C., Yuan, G. D., Bi, D. X., Xiao, L., Theng, B. K. G., et al. (2019b). Carbon-coated montmorillonite nanocomposite for the removal of chromium (VI) from aqueous solutions. *Journal of Hazardous Materials, 368,* 541–549.

Wei, J., Tu, C., Yuan, G. D., Liu, Y., Bi, D. X., Xiao, L., et al. (2019c). Assessing the effect of pyrolysis temperature on the molecular properties and copper sorption capacity of a halophyte biochar. *Environmental Pollution, 251,* 56–65.

Wu, P., Ata-Ul-Karim, S. T., Singh, B. P., Wang, H. L., Wu, T. L., Liu, C., et al. (2019). A scientometric review of biochar research in the past 20 years (1998–2018). *Biochar, 1*(1), 23–43.

Xiao, X., Chen, B. L., & Zhu, L. Z. (2014). Transformation, morphology, and dissolution of silicon and carbon in rice straw-derived biochar under different pyrolytic temperatures. *Environmental Science and Technology, 48*(6), 3411–3419.

Xiao, L., Wei, J., Yuan, G. D., Bi, D. X., Wang, J., Feng, L. R., et al. (2019a). Biochars made in the field using coupled oxygen-limiting and mist spraying technique and their properties. *Journal of Southwest University (Natural Science Edition), 41*(6), 15–20.

Xiao, L., Yuan, G. D., Bi, D. X., Wei, J., & Shen, G. H. (2019b). Equipment and technology of field preparation of biochars from agricultural and forest residues under aerobic conditions with water-fire coupled method. *Transactions of the Chinese Society of Agricultural Engineering, 35*(11), 239–244.

Yang, L., Bian, X. G., Yang, R. P., Zhou, C. L., & Tang, B. P. (2018). Assessment of organic amendment for improving coastal saline soil. *Land Degradation and Development, 29*(2), 3204–3211.

Yuan, S., Zhao, L. X., Meng, H. B., & Shen, Y. J. (2016). The main types of biochar and their properties and expectative researches. *Journal of Plant Nutrition and Fertilizer, 22*(5), 1402–1417.

Zhang, G. X., Liu, X. T., Sun, K., He, Q. H., Qian, T. W., & Yan, Y. L. (2013). Interactions of simazine, metsulfuron-methyl, and tetracycline with biochar and soil as a function of molecular structure. *Journal of Soils and Sediments, 13*(9), 1600–1610.

Zhang, J. H., & Wang, S. (2018). Trace for the motivations of the coalminers' off-site behaviors based on the evolutionary game theory. *Journal of Safety and Environment, 18*(2), 657–663.

Zhou, Q., Houge, B. A., Tong, Z., Gao, B., & Liu, G. (2018). An in situ technique for producing low-cost agricultural biochar. *Pedosphere, 28*(4), 690–695.